

## A novel family illustrating the mild phenotypic spectrum of *TUBB2B* variants



Jordy Dekker<sup>a</sup>, Karin E.M. Diderich<sup>a</sup>, Rachel Schot<sup>a</sup>, Sofie C. Husen<sup>b</sup>,  
Marjolein H.G. Dremmen<sup>c</sup>, Attie T.J.I. Go<sup>b</sup>, Marjolein J.A. Weerts<sup>a</sup>,  
Marjon A. van Slegtenhorst<sup>a</sup>, Grazia M.S. Mancini<sup>a,\*</sup>

<sup>a</sup> Department of Clinical Genetics, Erasmus MC University Medical Center, 3015, GD Rotterdam, the Netherlands

<sup>b</sup> Department of Obstetrics and Prenatal Medicine, Erasmus MC University Medical Center, 3015, GD Rotterdam, the Netherlands

<sup>c</sup> Department of Radiology and Nuclear Medicine, Erasmus MC University Medical Center, 3015, GD Rotterdam, the Netherlands

### ARTICLE INFO

#### Article history:

Received 30 April 2021

Received in revised form

12 August 2021

Accepted 9 September 2021

#### Keywords:

*TUBB2B* protein

Tubulin

Malformations of cortical development

Microtubules

### ABSTRACT

*TUBB2B* codes for one of the isoforms of  $\beta$ -tubulin and dominant negative variants in this gene result in distinctive malformations of cortical development (MCD), including dysgyria, dysmorphic basal ganglia and cerebellar anomalies. We present a novel family with a heterozygous missense variant in *TUBB2B* and an unusually mild phenotype. First, at 21<sup>3/7</sup> weeks of gestation ultrasonography revealed a fetus with a relatively small head, enlarged lateral ventricles, borderline hypoplastic cerebellum and a thin corpus callosum. The couple opted for pregnancy termination. Exome sequencing on fetal material afterwards identified a heterozygous maternally inherited variant in *TUBB2B* (NM\_178012.4 (*TUBB2B*):c.530A > T, p.(Asp177Val)), not present in GnomAD and predicted as damaging. The healthy mother had only a language delay in childhood. This inherited *TUBB2B* variant prompted re-evaluation of the older son of the couple, who presented with a mild delay in motor skills and speech. His MRI revealed mildly enlarged lateral ventricles, a thin corpus callosum, mild cortical dysgyria, and dysmorphic vermis and basal ganglia, a pattern typical of tubulinopathies. This son finally showed the same *TUBB2B* variant, supporting pathogenicity of the *TUBB2B* variant. These observations illustrate the wide phenotypic heterogeneity of tubulinopathies, including reduced penetrance and mild expressivity, that require careful evaluation in pre- and postnatal counseling.

© 2021 The Authors. Published by Elsevier Ltd on behalf of European Paediatric Neurology Society. This is an open access article under the CC BY license (<http://creativecommons.org/licenses/by/4.0/>).

### 1. Introduction

Cortical development of the human brain is a complex process, characterized by three main phases: neurogenesis, neuronal migration and cortical organization. Correct functioning of microtubules is indispensable for cortical development, since microtubules are key players in the mitotic spindle, organelle transport and cellular/neuron migration [1]. The cylindrical-growth of microtubules is determined by polymerization of  $\alpha$ - and  $\beta$ -tubulin heterodimers, which are encoded by several tubulin homologues. So far, variants in seven tubulin genes have been associated with an overlapping range of malformations of cortical development (MCD), regarding *TUBA1A* ( $\alpha$ -tubulin), *TUBB2A*, *TUBB2B*, *TUBB3*,

*TUBB4A*, *TUBB* (all  $\beta$ -tubulin types) and *TUBG1* ( $\gamma$ -tubulin) [2,3]. The overlapping but broad spectrum of MCDs caused by variants in these seven tubulin genes are referred to as “tubulinopathies”.

*TUBB2B* (OMIM:612850) is one of the  $\beta$ -tubulin isoforms, which is highly expressed in adult human brain [4]. During cortical development in mice *Tubb2b* is expressed in neural progenitors and post-mitotic migrating neurons, while in postnatal mouse brain *Tubb2b* expression is limited to macroglia [5]. To date over 40 pathogenic variants in *TUBB2B* have been reported, of which the majority are heterozygous *de novo* missense variants (reviewed in Suppl Table 1). Pathogenic variants in *TUBB2B* were first identified to result in asymmetric predominantly anterior polymicrogyria [6]. Revision of the cortical malformation in multiple cases led to the reclassification of the malformation as tubulin-related dysgyria [7]. Later, extension of the spectrum reported variable pachygyria, lissencephaly, dysmorphic basal ganglia, cerebellar vermis dysplasia, dysgenesis or agenesis of corpus callosum and brainstem

\* Corresponding author. Department of Clinical Genetics, Erasmus Medical Center, room Ee2077, Doctor Molewaterplein 40. 3015, GD Rotterdam, the Netherlands.  
E-mail address: [g.mancini@erasmusmc.nl](mailto:g.mancini@erasmusmc.nl) (G.M.S. Mancini).

**Table 1**  
Overview imaging and clinical phenotypes of three affected individuals in family.

Individual	Mother	Son	Fetus
Current age	30 y	5 y	N.A.
Sex	F	M	M
Variant	c.530A > T p.(Asp177Val)	c.530A > T p.(Asp177Val)	c.530A > T p.(Asp177Val)
Age at time of MRI	N.A.	3y 7mo	21 5/7 GW
Gyral pattern (location)	N.A.	Dysgyria (parieto-occipital)	Ventral and dorsal horns borderline normal
Basal ganglia	N.A.	Dysgenetic anterior limbs of capsula interna	N.A.
Cerebellum	N.A.	Vermis hypo- and dysplasia	Vermis hypoplasia
Corpus callosum	N.A.	Hypoplastic	Hypoplastic
Brain stem	N.A.	Normal	Normal
OFC last examination	−0.7 SD	0.71 SD (−1.65 SD at birth)	−1.2 SD
Motor development	Normal	Delayed	N.A.
Speech development	Delayed in childhood	Delayed	N.A.
Epilepsy	No	No	N.A.

N.A., not available; SD, standard deviation; y, year; mo, month; GW, gestational week

hypoplasia [3,6,8–26]. Affected individuals can present with a variable combination of epilepsy, mild to severe intellectual disability, behavioral issues and delayed/abnormal motor skills, including eye movements in congenital fibrosis of extraocular muscles, myoclonus-dystonia and Uner Tan syndrome (Suppl Table 1) [3,6,8–26]. We report three family members carrying a novel *TUBB2B* variant, with a phenotype at the very mild end of the spectrum.

## 2. Material and methods

Informed consent for all diagnostic tests was acquired. DNA was extracted from amniocytes and blood. Sanger-, exome sequencing and variant analysis was performed according to Ref. [27]. The analysis focused on a panel of 1178 genes involved in intellectual disability (NGS ID panel). For Sanger sequencing, first a PCR was performed with forward primer 5′-3′: CTTTGTGGGGCAACATCT and reverse primer 5′-3′: ACAGGCAACAGTGAAGAGCA, followed by a nested PCR with forward primer 5′-3′: ATTTAACGTTGGC-CATTTTG and reverse primer 5′-3′: CATGTTACCGCCAGCTT containing a M13 tail for sequencing. Pathogenicity of the variant was evaluated using Alamut Visual software (v2.15) and included screening for presence in a control population with the GnomAD online tool (gnomAD; <https://gnomad.broadinstitute.org>) and missense prediction tools: Align GVGD, Polyphen2, MutationTaster and SIFT [28–32]. Reference sequence according to NM\_178012.4 for *TUBB2B*.

## 3. Results

Advanced ultrasound at 21 3/7 gestational week (GW) of a 29 year old healthy pregnant woman (G2P1) revealed a fetus with a small head circumference (head circumference = 173,6 mm; p0.7, abdominal circumference = 163,6 mm; p38.4, femur length = 34,1 mm; p18.8) (Fig. 1A) [33]. Additional 2D and 3D neurosonogram revealed enlarged ventral horns of the lateral ventricles, posterior horns of the lateral ventricles within normal range (9,4 mm), a cavum vergae, small cerebellum (transcerebellar diameter = 20,6 mm; p7.6), with small dimensions of the vermis and a thin corpus callosum (height = 1,7 mm; <p5) (Fig. 1B) [34,35]. Also, gyration pattern was suspected to be lagging. Neurosonography was repeated at 22 6/7 GW and confirmed previous findings.

A fetal MRI performed at 21 5/7 GW revealed similar abnormalities, however less pronounced (Fig. 1A,B,C,D). The dorsal and ventral horns were borderline normal with a diameter of 9 and

6 mm, respectively (Fig. 1C and Suppl. Fig. 1A and B). Furthermore, the ventral horns had a plump morphology (Fig. 1C and Suppl. Fig. 1A and B). The height of the cerebellar vermis was 6 mm, which is small for the gestational age (Fig. 1D and Suppl. Fig. 1C and D). These abnormalities with uncertainty about prognosis made the couple decide to terminate the pregnancy.

Postmortem examination of the fetus revealed a small neurocranium and brain (no percentile known), with a relatively thin cortex resulting in ventriculomegaly, a thin corpus callosum and no overt cerebellar anomalies. Trio whole exome sequencing identified a novel heterozygous missense variant in exon 4 of the NM\_178012.4 (*TUBB2B*):c.530A > T, p.(Asp177Val) gene, inherited from the mother. This variant was not present in the GnomAD database, and predicted to be damaging *in silico* [28–32].

The mother's parents were tested and did not carry the *TUBB2B* variant. The mother had a speech delay in childhood, however is currently asymptomatic and has a head circumference within normal range (−0.7 SD), hence no brain MRI was performed (Table 1).

The older son of the couple had been referred to the pediatric neurologist at the age of 2.5 years because of a global developmental delay. The pediatric neurologist reported mild atrophy of the left calf muscles and hyporeflexia of the left Achilles tendon, resulting in disturbed gait and balance. Speech development was delayed and head circumference was within normal range (0,71 SD) (Table 1). The child was born by cesarean section with low Apgars (1/2-7-8 at 1, 5 and 10 min). The abnormalities found on brain MRI performed at 3 year and 7 months were initially interpreted as non-specific and possibly related to perinatal asphyxia. After the second pregnancy, DNA analysis of the boy showed the same heterozygous variant in *TUBB2B*. Revision of his brain MRI at the age of 4 year and 6 months revealed enlarged lateral ventricles with loss of periventricular white matter, a thin corpus callosum, bilateral dysgenetic anterior limbs of the capsula interna and a distortion of the striatum (R > L) and mild dysgyria of the cerebral cortex (Fig. 1E and F). Furthermore, hypoplasia and dysplasia of the cerebellar vermis with asymmetric foliation was seen on the brain MRI (Fig. 1F,G,H).

In the suspicion of a mosaic variant in the mother, the raw exome sequence data was reanalyzed and showed a mutant allele frequency of 40%, which cannot prove the presence of mosaicism.

## 4. Discussion

We identified a novel probably pathogenic heterozygous missense variant in *TUBB2B* (c.530A > T, p.(Asp177Val)) with a different presentation in three individuals within one family.

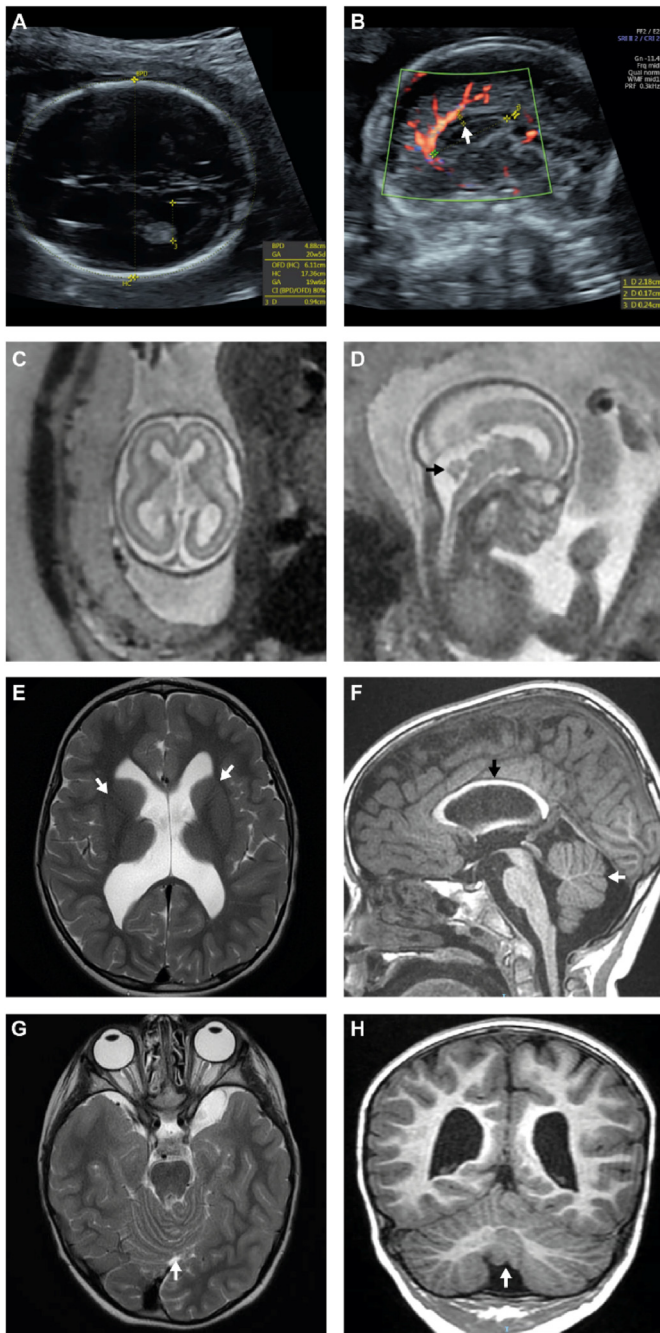


**Fig. 1.** Ultrasound and MRI fetus and brother. Advanced neurosonography at 21 3/7 GW and MRI at 21 5/7 GW of second child in utero (A–D). Postnatal MRI performed at age of 3 year and 7 months of first son (E–H). (A) Biparietal diameter (BPD) and head circumference (HC) are small for gestational age. (B) Body of corpus callosum is thin (1.7 mm; white arrow). (C) Axial T2-weighted image at the level of the lateral ventricles, ventral horns (6 mm) and dorsal horns (9 mm) size are borderline normal with a plump morphology. (D) Sagittal T2-weighted image in the midline, height of the cerebellar vermis is small for the gestational age (height: 6 mm; black arrow). (E) Axial T2-weighted image at the level of the lateral ventricles shows mild dysgyria, ex vacuo dilatation of lateral ventricles, bilateral dysgenetic anterior limbs of the capsula interna (white arrows) and reduced volume of the periventricular white matter. (F) Sagittal T1-weighted image in the midline reveals hypoplasia of cerebellar vermis (white arrow) and thin corpus callosum (black arrow). (G,H) Axial T2- and coronal T1-weighted image show dysplasia of cerebellar vermis with asymmetric foliation (white arrows). (For interpretation of the references to color in this figure legend, the reader is referred to the Web version of this article.)

After incorporation of an  $\alpha$ - and  $\beta$ -tubulin heterodimer into the microtubule, hydrolysis of the GTP to GDP in the  $\beta$ -tubulin destabilizes the microtubule lattice. Tubulin mutations affecting the GTP binding pocket seem to be often associated with a severe phenotype [3]. The Asp177 directly interacts by forming hydrogen bonds with the GTP/GDP, where the Val177 is no longer able to form these hydrogen bonds, due to its hydrophobic side chain (Fig. 2). The pathogenicity of the p.(Asp177Val) can be explained by decreased GTP/GDP binding and/or aberrant hydrolysis of the GTP. Two other studies reported a mild phenotype associated with a *TUBB2B* variant (p.Leu117Pro and p.Arg241His) not located in one of the GTP/GDP-binding amino acid residues [9,16,36]. Variants in *TUBB2B* have been identified throughout the gene, indicating that several variants can alter different aspects of tubulin and microtubule function [36]. However, the p.(Asp177Val) variant is the first to affect one of the eight amino acid residues (Gln11, Cys12, Ser138, Gly142, Thr143, Asp177, Asn204 and Asn226) that are known to form hydrogen bonds with the GTP/GDP and noteworthy leads to a milder phenotype (36; <https://www.rcsb.org/>, protein ID: 1JFF).

While it is difficult to predict the disease severity of the fetus, the clinical phenotype of the p.(Asp177Val) variant in the living individuals is typical for the variability observed for tubulinopathies at the mild end of the spectrum. The mother had only a speech delay during childhood and is currently asymptomatic. The 5 year old son has a moderate motor and language delay and the brain MRI revealed subtle but distinctive abnormalities, typical of a mild tubulinopathy.

Familiarity and interindividual variation of phenotypes within one family have been reported before [8,19]. One family has been described where the mother is more mildly affected than her daughters [8]. This suggests the influence of modifying factors on the phenotypic expression, although some cases are explained by the occurrence of somatic mosaicism in an apparently unaffected parent (Suppl Table 1) [15,19]. The MRI phenotype of the terminated pregnancy is also compatible with subtle tubulinopathy [3,14,20,25]. Literature review shows for *TUBB2B*, among tubulinopathies, very few familial cases and fetal diagnoses [3,8,14,15,19,23,25]. Besides cases with fetal akinesia and micro-lissencephaly, the most common fetal abnormalities, such as agenesis of corpus callosum and vermis hypoplasia, are rather non-specific and do not correlate to the severity of postnatal phenotype, making prenatal counseling difficult [3,14,25].

A possible explanation of the non-penetrant phenotype in the mother would be that she is a somatic mosaic, but she did not consent to further investigation. Literature review shows that inheritance from an asymptomatic parent occurs only in the presence of mosaicism [15,19]. However, there is a possibility that the mother is truly non-penetrant. For *CRADD*, a homozygous null variant has been described in a healthy father with hypogyration on MRI, where prenatal ultrasound revealed brain abnormalities in two fetuses, which led to termination of both pregnancies [37]. This literature example and our observation elucidate the importance of segregation analysis for a novel identified variant to predict the severity of prenatal brain abnormalities.

In conclusion, literature review and this report indicate that tubulinopathies caused by *TUBB2B* variants can present with a broad phenotypic spectrum, including very mild phenotype, even within one family. Such mild cases are more likely to remain undiagnosed and can complicate prenatal counseling of structural brain abnormalities.



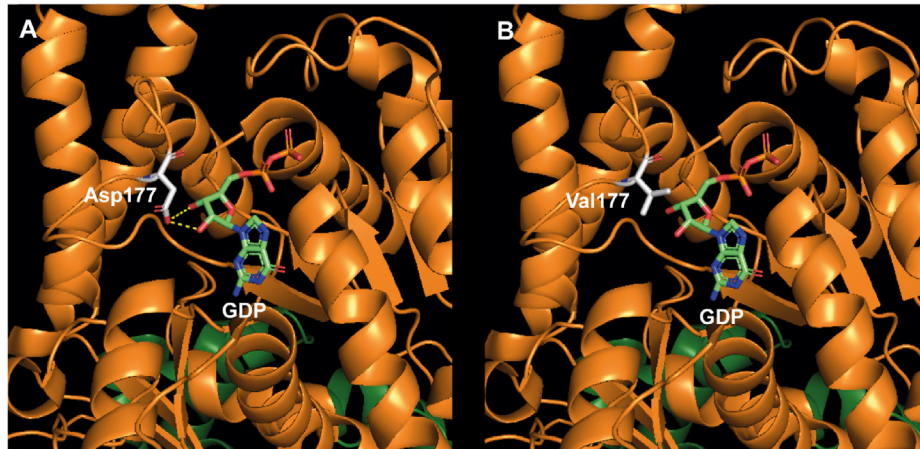


**Fig. 2.** 3D-modelling TUBB2B. (A,B) Dark-green:  $\alpha$ -tubulin, Orange:  $\beta$ -tubulin. (A) The acidic side chain of the Asp177 residue in  $\beta$ -tubulin forms hydrogen bonds with the GTP/GDP. (B) The Val177 variant present in our family is no longer able to form hydrogen bonds with the GTP/GDP, due to its hydrophobic side chain. 3D-modelling was performed with PyMOL V2.3.3 software using protein ID 1JFF from the RCSB protein data bank: <https://www.rcsb.org/> (For interpretation of the references to color in this figure legend, the reader is referred to the Web version of this article.)

**Funding**

This research did not receive any specific grant from funding agencies in the public, commercial, or not-for-profit sectors. GMSM is chair of the Neuro-MIG, European Network on Brain Malformations, supported by the COST Action CA16118.

**Data availability statement**

Data available on request from the authors.

**Declaration of competing interest**

None.

**Acknowledgments**

We thank Professor Bill Dobyns for fruitful discussion and the family members for their collaboration.

**Appendix A. Supplementary data**

Supplementary data to this article can be found online at <https://doi.org/10.1016/j.ejpn.2021.09.007>.

**References**

[1] Y. Feng, C.A. Walsh, Protein-protein interactions, cytoskeletal regulation and neuronal migration, *Nat. Rev. Neurosci.* 2 (2001) 408–416.  
 [2] R. Romaniello, F. Arrigoni, A.E. Fry, et al., Tubulin genes and malformations of cortical development, *Eur. J. Med. Genet.* 61 (2018) 744–754.  
 [3] N. Bahi-Buisson, K. Poirier, F. Fourniol, et al., The wide spectrum of tubulinopathies: what are the key features for the diagnosis? *Brain* 137 (2014) 1676–1700.  
 [4] L.J. Leandro-Garcia, S. Leskela, I. Landa, et al., Tumoral and tissue-specific expression of the major human beta-tubulin isoforms, *Cytoskeleton (Hoboken)* 67 (2010) 214–223.  
 [5] M. Breuss, J. Morandell, S. Nimpf, et al., The expression of *Tubb2b* undergoes a developmental transition in murine cortical neurons, *J. Comp. Neurol.* 523 (2015) 2161–2186.  
 [6] X.H. Jaglin, K. Poirier, Y. Saillour, et al., Mutations in the beta-tubulin gene *TUBB2B* result in asymmetrical polymicrogyria, *Nat. Genet.* 41 (2009) 746–752.  
 [7] R. Oegema, T.S. Barakat, M. Wilke, et al., International consensus recommendations on the diagnostic work-up for malformations of cortical development, *Nat. Rev. Neurol.* 16 (2020) 618–635.  
 [8] G.Y. Cederquist, A. Luchniak, M.A. Tischfield, et al., An inherited *TUBB2B*

mutation alters a kinesin-binding site and causes polymicrogyria, CFEOM and axon dysinnervation, *Hum. Mol. Genet.* 21 (2012) 5484–5499.  
 [9] R. Guerrini, D. Mei, D.M. Cordelli, et al., Symmetric polymicrogyria and pachygyria associated with *TUBB2B* gene mutations, *Eur. J. Hum. Genet.* 20 (2012) 995–998.  
 [10] R. Romaniello, A. Tonelli, F. Arrigoni, et al., A novel mutation in the beta-tubulin gene *TUBB2B* associated with complex malformation of cortical development and deficits in axonal guidance, *Dev. Med. Child Neurol.* 54 (2012) 765–769.  
 [11] T.D. Cushion, W.B. Dobyns, J.G. Mullins, et al., Overlapping cortical malformations and mutations in *TUBB2B* and *TUBA1A*, *Brain* 136 (2013) 536–548.  
 [12] D. Amrom, I. Tanyalcin, H. Verhelst, et al., Polymicrogyria with dysmorphic basal ganglia? Think tubulin!, *Clin. Genet.* 85 (2014) 178–183.  
 [13] R. Romaniello, F. Arrigoni, A. Cavallini, et al., Brain malformations and mutations in alpha- and beta-tubulin genes: a review of the literature and description of two new cases, *Dev. Med. Child Neurol.* 56 (2014) 354–360.  
 [14] C. Fallet-Bianco, A. Laquerriere, K. Poirier, et al., Mutations in tubulin genes are frequent causes of various foetal malformations of cortical development including microlissencephaly, *Acta Neuropathol Commun* 2 (2014) 69.  
 [15] R. Oegema, T.D. Cushion, I.G. Phelps, et al., Recognizable cerebellar dysplasia associated with mutations in multiple tubulin genes, *Hum. Mol. Genet.* 24 (2015) 5313–5325.  
 [16] J.T. Geiger, A.B. Schindler, C. Blauwendraat, et al., *TUBB2B* mutation in an adult patient with myoclonus-dystonia, *Case Rep Neurol* 9 (2017) 216–221.  
 [17] H. Wang, S. Li, S. Li, et al., De novo mutated *TUBB2B* associated pachygyria diagnosed by medical exome sequencing and long-range PCR, *Fetal Pediatr. Pathol.* 38 (2019) 63–71.  
 [18] J. Jimenez, D.A. Herrera, S.A. Vargas, et al., beta-Tubulinopathy caused by a mutation of the *TUBB2B* gene: magnetic resonance imaging findings of the brain, *Neuroradiol. J.* 32 (2019) 148–150.  
 [19] S. Citli, E. Serdaroglu, Maternal germline mosaicism of a de novo *TUBB2B* mutation leads to complex cortical dysplasia in two siblings, *Fetal Pediatr. Pathol.* (2020) 1–11.  
 [20] A. Laquerriere, M. Gonzales, Y. Saillour, et al., De novo *TUBB2B* mutation causes fetal akinesia deformation sequence with microlissencephaly: an unusual presentation of tubulinopathy, *Eur. J. Med. Genet.* 59 (2016) 249–256.  
 [21] R. Romaniello, F. Arrigoni, E. Panzeri, et al., Tubulin-related cerebellar dysplasia: definition of a distinct pattern of cerebellar malformation, *Eur. Radiol.* 27 (2017) 5080–5092.  
 [22] S.S. Jamuar, A.T. Lam, M. Kircher, et al., Somatic mutations in cerebral cortical malformations, *N. Engl. J. Med.* 371 (2014) 733–743.  
 [23] M.W. Breuss, T. Nguyen, A. Srivatsan, et al., Uner Tan syndrome caused by a homozygous *TUBB2B* mutation affecting microtubule stability, *Hum. Mol. Genet.* 26 (2017) 258–269.  
 [24] A. Accogli, M. Severino, A. Riva, et al., Targeted re-sequencing in malformations of cortical development: genotype-phenotype correlations, *Seizure* 80 (2020) 145–152.  
 [25] S. Cabet, K. Karl, C. Garel, et al., Two different prenatal imaging cerebral patterns of tubulinopathy, *Ultrasound Obstet. Gynecol.* 57 (2021) 493–497.  
 [26] C.A. Stutterd, S. Brock, K. Stouffs, et al., Genetic heterogeneity of polymicrogyria: study of 123 patients using deep sequencing, *Brain Commun* 3 (2021) fcaa221.  
 [27] L.V. Vandervore, R. Schot, E. Kasteleijn, et al., Heterogeneous clinical phenotypes and cerebral malformations reflected by rotatin cellular dynamics, *Brain* 142 (2019) 867–884.  
 [28] J.M. Schwarz, D.N. Cooper, M. Schuelke, et al., MutationTaster2: mutation

- prediction for the deep-sequencing age, *Nat. Methods* 11 (2014) 361–362.
- [29] N.L. Sim, P. Kumar, J. Hu, et al., SIFT web server: predicting effects of amino acid substitutions on proteins, *Nucleic Acids Res.* 40 (2012) W452–W457.
- [30] I.A. Adzhubei, S. Schmidt, L. Peshkin, et al., A method and server for predicting damaging missense mutations, *Nat. Methods* 7 (2010) 248–249.
- [31] S.V. Tavtigian, A.M. Deffenbaugh, L. Yin, et al., Comprehensive statistical study of 452 BRCA1 missense substitutions with classification of eight recurrent substitutions as neutral, *J. Med. Genet.* 43 (2006) 295–305.
- [32] M. Lek, K.J. Karczewski, E.V. Minikel, et al., Analysis of protein-coding genetic variation in 60,706 humans, *Nature* 536 (2016) 285–291.
- [33] B.O. Verburg, E.A. Steegers, M. De Ridder, et al., New charts for ultrasound dating of pregnancy and assessment of fetal growth: longitudinal data from a population-based cohort study, *Ultrasound Obstet. Gynecol.* 31 (2008) 388–396.
- [34] S. Pashaj, E. Merz, S. Wellek, Biometry of the fetal corpus callosum by three-dimensional ultrasound, *Ultrasound Obstet. Gynecol.* 42 (2013) 691–698.
- [35] Z. Leibovitz, C. Shkolnik, K.K. Haratz, et al., Assessment of fetal midbrain and hindbrain in mid-sagittal cranial plane by three-dimensional multiplanar sonography. Part 2: application of nomograms to fetuses with posterior fossa malformations, *Ultrasound Obstet. Gynecol.* 44 (2014) 581–587.
- [36] J. Lowe, H. Li, K.H. Downing, et al., Refined structure of alpha beta-tubulin at 3.5 Å resolution, *J. Mol. Biol.* 313 (2001) 1045–1057.
- [37] T. Harel, N. Hacoen, A. Shaag, et al., Homozygous null variant in CRADD, encoding an adaptor protein that mediates apoptosis, is associated with lissencephaly, *Am. J. Med. Genet.* 173 (2017) 2539–2544.